ЖЭТФ, 2013, том 143, вып. 5, стр. 977–983

STRONGLY CORRELATED QUANTUM SPIN LIQUID IN HERBERTSMITHITE

V. R. Shaginyan [a*], ***K. G. Popov*** [b], ***V. A. Khodel*** [c,d]

[a] *Petersburg Nuclear Physics Institute*
188300, Gatchina, Russia

[b] *Komi Science Center, Ural Branch of Russian Academy of Sciences*
167982, Syktyvkar, Russia

[c] *Russian Research Centre Kurchatov Institute*
123182, Moscow, Russia

[d] *McDonnell Center for the Space Sciences and Department of Physics, Washington University*
MO 63130, St. Louis, USA

Статья написана по материалам доклада
на 36-м Совещании по физике низких температур
(Санкт-Петербург, 2–6 июля 2012 г.)

Strongly correlated Fermi systems are among the most intriguing and fundamental systems in physics. We show that the herbertsmithite $ZnCu_3(OH)_6Cl_2$ can be regarded as a new type of strongly correlated electrical insulator that possesses properties of heavy-fermion metals with one exception: it resists the flow of electric charge. We demonstrate that herbertsmithite's low-temperature properties are defined by a strongly correlated quantum spin liquid made with hypothetic particles such as fermionic spinons that carry spin 1/2 and no charge. Our calculations of its thermodynamic and relaxation properties are in good agreement with recent experimental facts and allow us to reveal their scaling behavior, which strongly resembles that observed in heavy-fermion metals. Analysis of the dynamic magnetic susceptibility of strongly correlated Fermi systems suggests that there exist at least two types of its scaling.

DOI: 10.7868/S0044451013050236

Strongly correlated Fermi systems represented by heavy-fermion (HF) metals are well studied experimentally but received an adequate theoretical description only recently [1]. The Landau Fermi liquid (LFL) theory is highly successful in the condensed matter physics. The key point of this theory is the existence of fermionic quasiparticles defining the thermodynamic, relaxation, and dynamic properties of conventional metals. But strongly correlated Fermi systems encompass a variety of systems that display behavior not easily understood within the Fermi liquid theory and called non-Fermi-liquid (NFL) behavior. A paradigmatic example of the NFL behavior is demonstrated by HF metals, where a quantum phase transition (QPT) induces a transition between LFL and NFL [1, 2]. QPT can be tuned by different parameters, such as the chemical composition, the pressure, and the magnetic field. Magnetic materials, and insulators in particular, are interesting subjects of study due to a quantum spin liquid (QSL) that may develop in them, defining their low-temperature properties. Exotic QSL is formed with hypothetic particles such as fermionic spinons, carrying spin 1/2 and no charge. A search for the materials is a challenge for condensed matter physics [3].

In zero and high magnetic fields B [4–13], the experimental studies of herbertsmithite $ZnCu_3(OH)_6Cl_2$ have discovered gapless excitations analogous to quasiparticle excitations near the Fermi surface in HF metals, indicating that $ZnCu_3(OH)_6Cl_2$ is the promising system to investigate its QPTs and QSLs [14–16]. The observed behavior of the thermodynamic properties of $ZnCu_3(OH)_6Cl_2$ strongly resembles that in HF metals because a simple kagome

*E-mail: vrshag@thd.pnpi.spb.ru

lattice has a dispersionless topologically protected branch of the spectrum with zero excitation energy [14, 17, 18]. This indicates that the QSL formed by the ideal kagome lattice and located near the fermion condensation quantum phase transition (FCQPT) can be considered a strongly correlated quantum spin liquid (SCQSL). This observation allows establishing a close connection between $ZnCu_3(OH)_6Cl_2$ with its SCQSL and HF metals whose HF system is located near the FCQPT and therefore exhibits a universal scaling behavior [1, 14, 15]. Thus, the FCQPT represents a QPT of $ZnCu_3(OH)_6Cl_2$ and both herbertsmithite and HF metals can be treated in the same framework, while SCQSL is composed of spinons, which, with zero charge and spin $\sigma = \pm 1/2$, occupy the corresponding Fermi sphere with the Fermi momentum p_F [1, 14–16].

In this paper, we show that both NFL and scaling behavior of strongly correlated Fermi systems such as HF metals and $ZnCu_3(OH)_6Cl_2$ can be described in the framework of the FCQPT theory. Analyzing experimental data obtained in measurements on strongly correlated Fermi systems with different microscopic properties, we have found that they demonstrate a universal NFL behavior. Our analysis of the dynamic magnetic susceptibility of strongly correlated Fermi systems suggests that there exist at least two types of scaling. We calculate the thermodynamic and relaxation properties of herbertsmithite and HF metals. The calculations are in good agreement with experimental data and allow detecting the low-temperature behavior of $ZnCu_3(OH)_6Cl_2$ defined by SCQSL as that observed in HF metals.

To study the low-temperature thermodynamic, relaxation, and scaling properties of herbertsmithite theoretically, we use the model of a homogeneous HF liquid [1]. This model permits avoiding complications associated with the crystalline anisotropy of solids. Similarly to the electronic liquid of HF metals, the SCQSL is composed of chargeless fermions (spinons) with $S = 1/2$ occupying the corresponding two Fermi spheres with the Fermi momentum p_F. The ground-state energy $E(n)$ is given by the Landau functional depending on the quasiparticle distribution function $n_\sigma(\mathbf{p})$, where p is the momentum and σ is the spin index. The effective mass M^* is governed by the Landau equation [1, 19]

$$\frac{1}{M^*(B,T)} = \frac{1}{M^*} + \frac{1}{p_F^2}\sum_{\sigma_1}\int \frac{\mathbf{p}_F\cdot\mathbf{p}_1}{p_F}\times \\ \times F_{\sigma,\sigma_1}(\mathbf{p}_F,\mathbf{p}_1)\frac{\partial\delta n_{\sigma_1}(\mathbf{p}_1,B,T)}{\partial p_1}\frac{d\mathbf{p}_1}{(2\pi)^3}, \quad (1)$$

where we write the quasiparticle distribution function as

$$n_\sigma(\mathbf{p},B,T) = n_\sigma(\mathbf{p},B=0,T=0) + \delta n_\sigma(\mathbf{p},B,T).$$

The Landau amplitude F is completely defined by the fact that the system has to be at a FCQPT [1, 20–22] (see [20–22] for details of solving Eq. (1)). The sole role of the Landau amplitude is to bring the system to the FCQPT point, where the Fermi surface alters its topology such that the effective mass acquires temperature and field dependences. At this point, the term $1/M^*$ vanishes, Eq. (1) becomes homogeneous and can be solved analytically [1, 20]. At $B = 0$, the effective mass, being strongly T-dependent, demonstrates the NFL behavior given by Eq. (1),

$$M^*(T) \approx a_T T^{-2/3}, \quad (2)$$

where a_T is a constant. At finite T, under the application of a magnetic field B, the two Fermi spheres due to the Zeeman splitting are displaced by opposite amounts, the final chemical potential μ remaining the same to within corrections of the order of B^2. As a result, the field B drives the system to the LFL region, and again it follows from Eq. (1) that

$$M^*(B) \approx a_B B^{-2/3}, \quad (3)$$

where a_B is a constant. It follows from Eqs. (2) and (3) that effective mass diverges at the FCQPT. At finite B and T, solutions $M^*(B,T)$ of Eq. (1) can be well approximated by a simple universal interpolating function. This interpolation occurs between the LFL regime, given by Eq. (3), and the NFL regime given by Eq. (2) [1, 20]. Experimental facts and calculations show that $M^*(B,T)$ as a function of T at a fixed B reaches its maximum value M^*_M at T_M (see, e. g., [1]).

To study the universal scaling behavior of strongly correlated Fermi systems, it is convenient to introduce the normalized effective mass M^*_N and the normalized temperature T_N by dividing the effective mass M^* and temperature T by their values at the maximum, M^*_M and T_M. In the same way, we can normalize other thermodynamic functions such as the spin susceptibility χ and the heat capacity C. As a result, we obtain

$$\chi_N \approx (C/T)_N \approx M^*_N, \quad (4)$$

where χ_N and $(C/T)_N$ are the normalized values of χ and C/T. We note that our calculations of M^*_N based on Eq. (1) do not contain any fitting parameters. The normalized effective mass

$$M^*_N = M^*/M^*_M$$

as a function of the normalized temperature

$$y = T_N = T/T_M$$

is given by the interpolating function [1]

$$M_N^*(y) \approx c_0 \frac{1 + c_1 y^2}{1 + c_2 y^{8/3}}, \quad (5)$$

where

$$c_0 = (1 + c_2)/(1 + c_1),$$

c_1, and c_2 are fitting parameters. Because the magnetic field B enters Eq. (1) only in the combination $B\mu_B/k_BT$, we have $T_{max} \propto B$ [20, 1], where μ_B is the Bohr magneton and k_B is the Boltzmann constant. Hence, for finite magnetic fields, the variable y becomes

$$y = T/T_M \propto k_BT/\mu_BB. \quad (6)$$

Because the variables T and B enter symmetrically, Eq. (5) is valid for

$$y = \mu_BB/k_BT.$$

To construct the dynamic spin susceptibility

$$\chi(\mathbf{q}, \omega, T) = \chi'(\mathbf{q}, \omega, T) + i\chi''(\mathbf{q}, \omega, T)$$

as a function of the momentum q, frequency ω, and temperature T, we again use the model of a homogeneous HF liquid located near the FCQPT. To deal with the dynamic properties of Fermi systems, we can use the transport equation describing a slowly varying disturbance $\delta n_\sigma(\mathbf{q}, \omega)$ of the quasiparticle distribution function $n_0(\mathbf{p})$, and $n = \delta n + n_0$. We consider the case where the disturbance is induced by the application of an external magnetic field

$$B = B_0 + \lambda B_1(\mathbf{q}, \omega)$$

with B_0 being a static field and λB_1 a ω-dependent field with $\lambda \to 0$. As long as the transferred energy

$$\omega < qp_F/M^* \ll \mu,$$

where M^* is the effective mass and μ is the chemical potential, the quasiparticle distribution function $n(\mathbf{q}, \omega)$ satisfies the transport equation [23]

$$(\mathbf{q}\cdot\mathbf{v}_p - \omega)\delta n_\sigma - \mathbf{q}\cdot\mathbf{v}_p \frac{\partial n_0}{\partial \varepsilon_p} \sum_{\sigma_1 \mathbf{p}_1} f_{\sigma,\sigma_1}(\mathbf{p}\cdot\mathbf{p}_1)\delta n_{\sigma_1}(\mathbf{p}_1) = = \mathbf{q}\cdot\mathbf{v}_p \frac{\partial n_0}{\partial \varepsilon_p} \sigma\mu_B(B_0 + \lambda B_1), \quad (7)$$

where μ_B is the Bohr magneton and ε_p is the single-particle spectrum. In the field B_0, the two Fermi surfaces are displaced by opposite amounts, $\pm B_0\mu_B$, and

$$\mathcal{M} = \mu_B(\delta n_+ - \delta n_-),$$

where the two spin orientations with respect to the magnetic field are denoted by "±" and the magnetization

$$\delta n_\pm = \sum_p \delta n_\pm(\mathbf{p}).$$

The spin susceptibility χ is given by

$$\chi = \left.\frac{\partial \mathcal{M}}{\partial B}\right|_{B=B_0}.$$

In fact, transport equation (7) reduces to two equations, which can be solved for each direction "±" and allow calculating $\delta n_\pm$ and the magnetization. The response to the application of $\lambda B_1(\mathbf{q}, \omega)$ can be found by expanding the solution of Eq. (7) in a power series with respect to $M^*\omega/qp_F$. As a result, we obtain the imaginary part of the spin susceptibility

$$\chi''(\mathbf{q}, \omega) = \mu_B^2 \frac{\omega(M^*)^2}{2\pi q} \frac{1}{(1 + F_0^a)^2}, \quad (8)$$

where F_0^a is the dimensionless spin-antisymmetric quasiparticle interaction [23]. The interaction F_0^a is found to saturate at $F_0^a \approx -0.8$ [24, 25], and therefore the factor $(1 + F_0^a)$ in Eq. (8) is finite and positive. It can be seen from Eq. (8) that the second term is an odd function of ω. Therefore, it does not contribute to the real part χ' and forms the imaginary part χ''. Taking into account that at relatively high frequencies

$$\omega \geq qp_F/M^* \ll \mu$$

in the hydrodynamic approximation, $\chi' \propto 1/\omega^2$ [26], we conclude that the expression

$$\chi(\mathbf{q}, \omega) = \frac{\mu_B^2}{\pi^2(1 + F_0^a)} \frac{M^*p_F}{1 + i\pi \dfrac{M^*\omega}{qp_F(1 + F_0^a)}}, \quad (9)$$

yields a simple approximation for the susceptibility χ and satisfies the Kramers–Kronig relation connecting the real and imaginary parts of χ.

To understand how χ'' and χ respectively given by Eqs. (8) and (9) can depend on the temperature T and magnetic field B, we recall that near the FCQPT point, the effective mass M^* depends on T and B. To elucidate the scaling behavior of χ, we use Eq. (2) to describe the temperature dependence of χ. It follows from Eqs. (9) and (2) that

$$T^{2/3}\chi(T, \omega) \approx \frac{a_1}{1 + ia_2E}, \quad (10)$$

where a_1 and a_2 are constants absorbing irrelevant values and

$$E = \omega/(k_B T)^{2/3}.$$

As a result, the imaginary part $\chi''(T,\omega)$ satisfies the equation

$$T^{2/3}\chi''(T,\omega) \approx \frac{a_3 E}{1 + a_4 E^2}, \qquad (11)$$

where a_3 and a_4 are constants. It follows from Eq. (11) that $T^{2/3}\chi''(T,\omega)$ has a maximum $(T^{2/3}\chi''(T,\omega))_{max}$ at some E_{max} and depends on the only variable E. Equation (11) is in accordance with the scaling behavior of $\chi'' T^{0.66}$ experimentally established in Ref. [7]. As it was done for the effective mass when constructing (5), we introduce the dimensionless function

$$(T^{2/3}\chi'')_N = T^{2/3}\chi''/(T^{2/3}\chi'')_{max}$$

and the dimensionless variable $E_N = E/E_{max}$, after which Eq. (11) becomes

$$(T^{2/3}\chi'')_N \approx \frac{b_1 E_N}{1 + b_2 E_N^2}, \qquad (12)$$

where b_1 and b_2 are fitting parameters to be chosen such that the function in the right-hand side of Eq. (12) reaches its maximum value 1 at $E_n = 1$.

We next construct the schematic $T - B$ phase diagram of $ZnCu_3(OH)_6Cl_2$ reported in Fig. 1. At $T = 0$ and $B = 0$, the system is near the FCQPT without tuning. It can also be shifted from the FCQPT by the application of a magnetic field B. The magnetic field B and temperature T play the role of control parameters, driving the system from the NFL to LFL regions as shown by the vertical and horizontal arrows. At a fixed B and increasing T, the system transits along the vertical arrow from the LFL region to the NFL one, crossing the transition region. On the contrary, increasing B at a fixed T drives the system along the horizontal arrow from the NFL region to the LFL one. The inset demonstrates the universal behavior of the normalized effective mass M_N^* versus the normalized temperature T_N given by Eq. (5). It follows from Eq. (5) and can be seen from Fig. 1 that the total width W of the NFL and the transition region, shown by the arrow in Fig. 1, tends to zero as T and B decrease, because $W \propto T \propto B$.

A few remarks are in order here. Equation (11) is valid if the system approaches the FCQPT from the disordered side as shown in phase diagram 1. If the system is located on the ordered side, then at $B = 0$

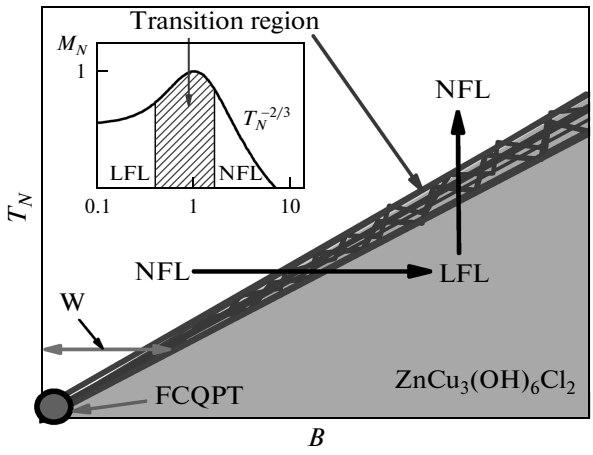

Рис. 1. Schematic T–B phase diagram of $ZnCu_3(OH)_6Cl_2$ located on the disordered side of the FCQPT. The solid circle at the origin shown by an arrow represents FCQPT. Vertical and horizontal arrows show the respective LFL–NFL and NFL–LFL transitions at fixed B and T. The total width W of the NFL and the transition region is shown by the arrow. The inset demonstrates the behavior of the normalized effective mass M_N^* versus the normalized temperature T_N given by Eq. (5). Temperatures $T_N \sim 1$ signify a transition region between the LFL regime with an almost constant effective mass and the NFL regime, given by an $T^{-2/3}$ dependence. The transition region, where M_N^* reaches its maximum at $T/T_{max} = 1$, is shown by the arrows and hatched area both in the main panel and in the inset

the behavior of the effective mass as a function of T is given by [1, 28]

$$M^*(T) \approx a_\tau T^{-1}, \qquad (13)$$

where a_τ is a constant. Taking Eq. (13) into account and proceeding in the same way as in deriving Eq. (11), we obtain that the imaginary part $\chi''(T,\omega)$ is given by

$$T\chi''(T,\omega) \approx \frac{a_5 E}{1 + a_6 E^2}, \qquad (14)$$

where a_5 and a_6 are constants and $E = \omega/k_B T$. It follows from Eq. (14) that $T\chi''(T,\omega)$ depends on the only variable E. Thus, Eqs. (11) and (14) establish two types of scaling behavior of $\chi''(\omega,T)$. Since the scaling behavior of $\chi''(\omega,T)$ is defined by the dependence of M^* on T, we can expect new types of scaling, especially in the transition region shown in Fig. 1.

Figure 2 reports the behavior of the normalized χ_N and specific heat $(C/T)_N$ respectively extracted from measurements on $ZnCu_3(OH)_6Cl_2$ [7] and $YbRh_2Si_2$

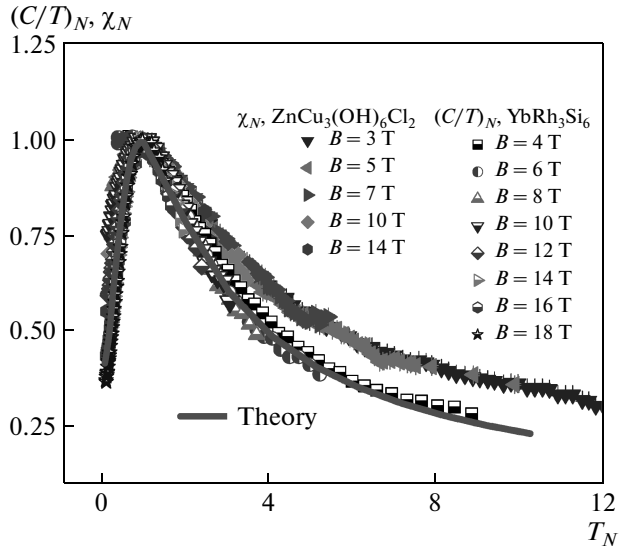

Рис. 2. The experimental data on measurements of $\chi_N \approx (C/T)_N \approx M_N^*$ and our calculations of M_N^* at fixed magnetic field are respectively shown in the legends by points of different shape and a solid curve. It is clearly seen that the data collected on both $ZnCu_3(OH)_6Cl_2$ [7] and $YbRh_2Si_2$ [27] merge into the same curve, obeying a scaling behavior. This demonstrates that the SCQSL of herbertsmithite is close to the FCQPT and behaves like an HF liquid of $YbRh_2Si_2$ in magnetic fields

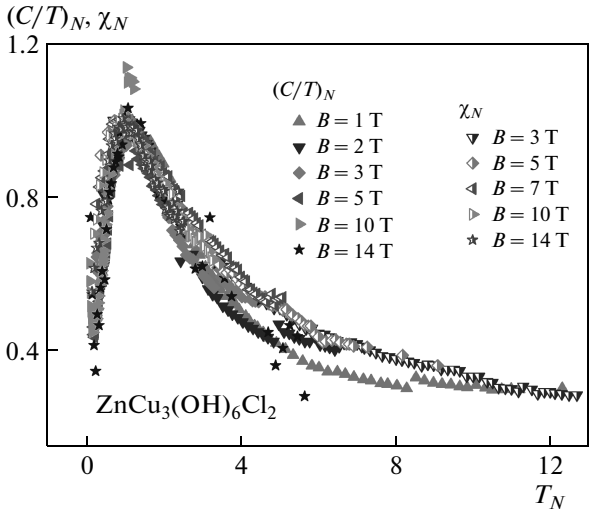

Рис. 3. The normalized susceptibility $\chi_N \approx M_N^*$ and the normalized specific heat $(C/T)_N \approx M_N^*$ of SCQSL versus the normalized temperature T_N as a function of the magnetic fields shown in the legends. χ_N and $(C/T)_N$ are respectively extracted from the data in [7] and [5]

[27]. It follows from Fig. 2 that in accordance with Eq. (4), the behavior of χ_N coincides with that of $(C/T)_N$ in $YbRh_2Si_2$.

In Fig. 3, the normalized χ_N and $(C/T)_N$, extracted from measurements on $ZnCu_3(OH)_6Cl_2$ [5, 7], are depicted. To extract the specific heat C coming from the contribution of SCQSL from the total specific heat $C_t(T)$ measured on $ZnCu_3(OH)_6Cl_2$, we approximate $C_t(T)$ at $T > 2$ K by the function [15]

$$C_t(T) = a_1 T^3 + a_2 T^{1/3}, \qquad (15)$$

where the first term proportional to a_1 is due to the lattice (phonon) contribution and the second is determined by the SCQSL when it exhibits the NFL behavior in accordance with Eq. (2),

$$C \propto TM^* \propto T^{1/3}.$$

Taking into account that the phonon contribution is B-field independent, we obtain

$$C(B,T) = C_t(B,T) - a_1 T^3.$$

It can be seen from Figs. 2 and 3 that

$$(C/T)_N \approx \chi_N$$

displays the same scaling behavior as $(C/T)_N$ measured on the HF metal $YbRh_2Si_2$. Therefore, the scaling behavior of the thermodynamic functions of herbertsmithite is an intrinsic feature of the compound.

In Fig. 4, consistent with Eq. (12), the scaling of the normalized dynamic susceptibility $(T^{2/3}\chi'')_N$ extracted from the inelastic neutron scattering spectrum of both herbertsmithite [7] (Fig. 4*a*), and the HF metal $Ce_{0.925}La_{0.075}Ru_2Si_2$ [29] (Fig. 4*b*), is displayed. In Fig. 4*c* the dynamic susceptibility $T\chi''$ extracted from measurements of the inelastic neutron scattering spectrum on the HF metal $YbRh_2Si_2$ [30] is shown. The data for $T\chi''$ exhibit the scaling behavior over three decades of the variation of both the function and the variable, thus confirming the validity of Eq. (14). The scaled data obtained in measurements on such quite different strongly correlated systems as $ZnCu_3(OH)_6Cl_2$, $Ce_{0.925}La_{0.075}Ru_2Si_2$, and $YbRh_2Si_2$ collapse fairly well onto a single curve over almost three decades of the scaled variables. Our calculations shown by the solid curves are in good agreement with the experimental facts.

Some remarks on the role of both the disorder and the anisotropy are in order. The anisotropy is supposed to be related to the Dzyaloshinskii–Moriya interaction, exchange anisotropy, or out-of-plane impurities. Measurements of the susceptibility on a single crystal

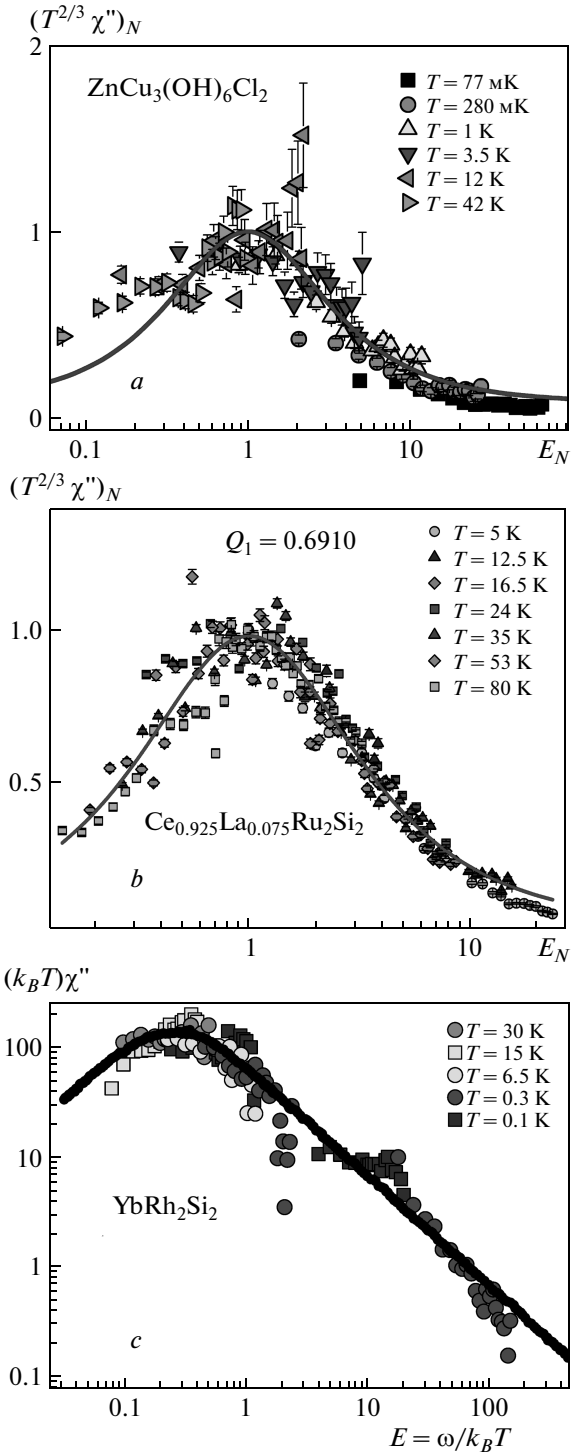

Рис. 4. Panels a and b: $(T^{2/3}\chi'')_N$ plotted against the dimensionless ratio $E_N = \omega/(k_BT)^{2/3}E_{max}$. The data are extracted from measurements on $ZnCu_3(OH)_6Cl_2$ [7] (a) and $Ce_{0.925}La_{0.075}Ru_2Si_2$ (b) at Q_1 [29]. The solid curves, panels a and b, are fits with the function given by Eq. (12). Panel c: $T\chi''$ plotted against $E = \omega/k_BT$. The data are extracted from measurements on $YbRh_2Si_2$ [30], with the function given by Eq. (14)

of herbertsmithite have shown that it closely follows that measured on a powder sample [8, 13]. At low temperatures $T \lesssim 70$ K, the single-crystal data do not show substantial magnetic anisotropy [8, 13]. It is seen from Figs. 2, 3, and 4 that in accordance with Eqs. (4) and (5), $(C_{mag}/T)_N \approx \chi_N$, and displays the same scaling behavior as does $(C/T)_N$ measured on the HF metal $YbRh_2Si_2$. These observations show that extra Cu spins outside the kagome planes regarded as paramagnetic weakly interacting impurities can hardly be responsible for both the scaling behavior and the divergence of the susceptibility. Indeed, in such a case, the extra Cu spins would be completely polarized by a relatively weak magnetic field, while the extra Cu spins do not contribute significantly to the specific heat. Hence, one could scarcely expect that the scaling behavior of $(C_{mag}/T)_N$ in magnetic fields should coincide with that of χ_N. On the other hand, as can be seen from Fig. 3, these functions exhibit the same scaling behavior. Moreover, it follows from Fig. 2 that the same scaling is demonstrated by $(C/T)_N$ obtained in measurements on $YbRh_2Si_2$. Therefore, our consideration evidences that the stoichiometry, disorder, and anisotropy contribute very little to the measurements on $ZnCu_3(OH)_6Cl_2$ at relatively low temperatures. These observations are in agreement with the general consideration of scaling behavior of HF metals in [1, 15].

In summary, we have considered the non-Fermi liquid behavior and the scaling behavior of strongly correlated Fermi systems such as insulator $ZnCu_3(OH)_6Cl_2$ and HF metals $Ce_{0.925}La_{0.075}Ru_2Si_2$ and $YbRh_2Si_2$, and shown that these are described in the framework of the FCQPT theory. Our analysis of the dynamic magnetic susceptibility of strongly correlated Fermi systems suggests that there exist at least two types of its scaling. We calculate the thermodynamic and relaxation properties of herbertsmithite and HF metals. The calculations are in good agreement with experimental data and allow identifying the low-temperature behavior of $ZnCu_3(OH)_6Cl_2$ determined by SCQSL as that observed in HF metals. Therefore, herbertsmithite can be regarded as a new type of strongly correlated electrical insulator that has the properties of HF metals with one exception: it resists the flow of electric charge.

KGP acknowledges funding from the Ural Branch of the Russian Academy of Sciences, basic research program № 12-U-1-1010, and the Presidium of the Russian Academy of Sciences, program № 12-P1-1014.

REFERENCES

1. V. R. Shaginyan, M. Ya. Amusia, A. Z. Msezane, and K. G. Popov, Phys. Rep. **492**, 31 (2010).
2. H. V. Löhneysen, A. Rosch, M. Vojta, and P. Wölfle, Rev. Mod. Phys. **79**, 1015 (2007).
3. L. Balents, Nature **464**, 199 (2010).
4. M. P. Shores, E. A. Nytko, B. M. Bartlett, and D. G. Nocera, J. Amer. Chem. Soc. **127**, 13462 (2005).
5. J. S. Helton, K. Matan, M. P. Shores et al., Phys. Rev. Lett. **98**, 107204 (2007).
6. M. A. deVries, K. V. Kamenev, W. A. Kockelmann et al., Phys. Rev. Lett. **100**, 157205 (2008).
7. J. S. Helton, K. Matan, M. P. Shores et al., Phys. Rev. Lett. **104**, 147201 (2010).
8. T. H. Han, J. S. Helton, S. Chu et al., Phys. Rev. B **83**, 100402(R) (2011).
9. F. Bert and P. Mendels, J. Phys. Soc. Jpn. **79**, 011001 (2010).
10. F. Mila, Phys. Rev. Lett. **81**, 2356 (1998).
11. S. S. Lee and P. A. Lee, Phys. Rev. Lett. **95**, 036403 (2005).
12. Y. Ran, M. Hermele, P. A. Lee, and X. G. Wen, Phys. Rev. Lett. **98**, 117205 (2007).
13. T. Han, S. Chu, and Y. S. Lee, Phys. Rev. Lett. **108**, 157202 (2012).
14. V. R. Shaginyan, A. Z. Msezane, and K. G. Popov, Phys. Rev. B **84**, 060401(R) (2011).
15. V. R. Shaginyan, A. Z. Msezane, K. G. Popov et al., Europhys. Lett. **97**, 56001 (2012).
16. V. R. Shaginyan, A. Z. Msezane, K. G. Popov, and V. A. Khodel, Phys. Lett. A **376**, 2622 (2012).
17. D. Green, L. Santos, and C. Chamon, Phys. Rev. B **82**, 075104 (2010).
18. T. T. Heikkila, N. B. Kopnin, and G. E. Volovik, JETP Lett. **94**, 233 (2011).
19. L. D. Landau, Sov. Phys. JETP **3**, 920 (1956).
20. J. W. Clark, V. A. Khodel, and M. V. Zverev, Phys. Rev. B **71**, 012401 (2005).
21. V. A. Khodel, J. W. Clark, and M. V. Zverev, Phys. Rev. B **78**, 075120 (2008).
22. V. R. Shaginyan, K. G. Popov, V. A. Stephanovich et al., Europhys. Lett. **93**, 17008 (2011).
23. D. Pines and P. Nozières, *Theory of Quantum Liquids*, Benjamin, New York (1966).
24. M. Pfitzner and P. Wölfle, Phys. Rev. B **33**, 2003 (1986).
25. D. Vollhardt, P. Wölfle, and P. W. Anderson, Phys. Rev. B **35**, 6703 (1987).
26. D. Forster, *Hydrodynamic Fluctuations, Broken Symmetry, and Correlation Functions*, Benjamin (1975).
27. P. Gegenwart, Y. Tokiwa, T. Westerkamp et al., New J. Phys. **8**, 171 2006.
28. V. A. Khodel and V. R. Shaginyan, JETP Lett. **51**, 553 (1990).
29. W. Knafo, S. Raymond, J. Flouquet et al., Phys. Rev. B **70**, 174401 (2004).
30. C. Stock, C. Broholm, F. Demmel et al., Phys. Rev. Lett. **109**, 127201 (2012).